JOURNAL OF MATERIALS SCIENCE 29 (1994) 4319–4324

The effect of sintering on the mechanical properties of SOFC ceramic interconnect materials

N. M. SAMMES, R. RATNARAJ
Centre for Technology, The University of Waikato, Private Bag 3105, Hamilton, New Zealand
M. G. FEE
Industrial Research Ltd, Gracefield Road, PO Box 31-310, Lower Hutt, New Zealand

Solid oxide fuel cell (SOFC) interconnect materials, strontium and calcium doped lanthanum chromite, were synthesized to investigate the effect of dopant content and sintering temperature on their sinterability. The results show that approximately 96% of the theoretical density could be achieved when $LaCrO_3$, doped with 30 mol% Ca, was sintered in air at 1400 °C. However, to get the same sintered density for the strontia doped material, a 1700 °C sintering temperature had to be used. The effect of sintering temperature on the fracture strength was also investigated. A maximum fracture strength of 234 MPa for $La_{0.7}Sr_{0.3}CrO_{3-\delta}$ and 256 MPa for $La_{0.7}Ca_{0.3}CrO_{3-\delta}$ were obtained for both samples sintered at 1700 °C.

1. Introduction

Solid oxide fuel cells (SOFC) are a promising new supply of clean efficient energy for electrical power generation. Planar SOFC systems offer distinct advantages over tubular designs especially in their ease of fabrication and higher power density [1, 2]. Planar solid oxide fuel cells are classified as being either self-supported or supported, and in both types a metal oxide or metallic interconnect (bipolar plate) is required to allow stacked systems to be developed [3]. The interconnect must possess high chemical stability in both reducing and oxidizing environments, high electronic conductivity, good sinterability and a thermal expansion coefficient similar to the adjoining cell components. Alkaline earth doped lanthanum chromites are thought to be the most promising candidate materials for the interconnect [3–5]. The interconnect for the planar system needs to have a large area and, in most designs, sufficient strength to support other cell components [5]. Thus, a lot of effort has been made to improve the sinterability of this component. However, many authors have reported that lanthanum chromites are very difficult to sinter in air due to the high vapour pressure of the chromium [5–8]. Several methods have been used to improve the sinterability including the addition of sintering aids (such as fluorides) [6], addition of dopant transition metals (such as Zn or Cu) [7], the use of reducing atmospheres and the effect of a slightly non-stoichiometric lanthanum chromite material [8]. Tai and Lessing [9] reported a theoretical density of above 93% for $La_{1-x}Sr_xCrO_3$, when sandwiched between two Cr_2O_3 plates and fired at 1700 °C for 7 h. Chick *et al.* [10] reported 93% densification for $La_{0.76}Sr_{0.24}CrO_3$ after sintering at 1550 °C. Ninety-five per cent theoretical dense $La_{1-x}Ca_xCr_{1-y}O_3$ was observed after firing at 1550 °C in air. It is generally accepted that strontium doped lanthanum chromite systems are more stable than the calcium doped systems. However, when a co-firing procedure is required the calcium doped lanthanum chromite has been used due to its lower sintering temperature [11]. However, at calcium contents above $x = 0.15$, in $La_xCa_{1-x}CrO_3$, CaO was found to precipitate causing a reduction in the electronic conductivity. La_2O_3 precipitation, at $x < 0.15$, was found to cause disintegration of the sample due to its hygroscopic nature. The formation of the second phases (CaO or La_2O_3) were, however, found to depress the vaporization of the chromium component from $La_{1-x}Ca_xCrO_3$, which in turn helps to sinter the material.

The effect of sinterability has been investigated in some detail, but the mechanical properties of these interconnect materials has not. Steele [12] has reported a value of approximately 300 MPa for the modulus of rupture of $LaCr_{0.8}Mg_{0.2}CrO_{3-\delta}$, however, detailed information about the sample was not reported. This work reports the effect of sintering temperature on the sinterability and mechanical properties of $La_{1-x}Sr_xCrO_3$ and $La_{1-x}Ca_xCrO_3$.

2. Experimental procedure

$La_{1-x}Sr_xCrO_3$ (LSC) and $La_{1-x}Ca_{1-x}CrO_3$ (LCC) ($x = 0$–0.3) were prepared from $CaCO_3$ (99.995%), $SrCO_3$ (99.995%), La_2O_3 (99.99%) and $Cr(NO_3)_3$ (99%) (Aldrich Chemicals). The samples were synthesized by two routes. Firstly, the standard solid state route involved ball milling (using FSZ as the milling media) the stoichiometric amounts of the required

0022–2461

powders in ethanol for 24 h. The sample was then heated to remove the ethanol and fired at 1500 °C for 5 h. Powder X-ray diffraction (XRD), using a Philips X-ray diffractometer, was undertaken to determine the formation of the perovskite phase. Continual firing was conducted to ensure that the reaction had gone to completion. The second synthesis route involved a wet chemical route using a polymeric precursor. This method was based on the modified Pechini route [13] and involved dissolving the required salts in concentrated nitric acid and water (to ensure polymerization). A 50:50 mol ratio of citric acid:ethylene glycol was then added and the whole heated to 95 °C, until polymerization had taken place. The sample was then charred at 300 °C and pulverized to form a fine particle size. Sintering was then undertaken at 900 °C for 5 h. The particle size of the powders was determined using a Malvern Particle size analyser. High temperature X-ray diffraction data was obtained in air using an Anton Paar HTK high temperature furnace mounted on a Philips PW1050 goniometer automated by a Sietronics SIE112 microprocessor using β-filtered cobalt radiation. Scanning electron microscopy was undertaken using a Hitatchi S4000 attached to a Kevex microanalyser system.

The powders were pressed into 10 mm diameter pellets of 1.5–2 mm thickness, compacted using a die press at 400 kg cm^{-2}. The pellets were pressed to allow the relative density measurements to be undertaken. Bars of 30 × 10 × 2 mm^3 were also die pressed at 400 kg cm^{-2}. The bars were used to measure the modulus of rupture of the interconnect material. In both cases densification was carried out over the temperature range of 1100 to 1700 °C, for 2–10 h in a SiC element furnace, with a slow heating and cooling rate of 5 °C min^{-1}. Sinterability was examined in terms of the relative density of the sintered pellet and was measured using the standard Archimedes principle method. Theoretical density (d_0) was calculated using experimental lattice parameters and the chemical formula $La_{1-x}Ca_xCrO_3$ and $La_{1-x}Sr_xCrO_3$. The fracture strength (modulus of rupture) was measured using a three-point bend test, with a distance of 24 mm between the points of contact, using an Instron 4204 tensile testing machine interfaced to an IBM computer. A minimum of five tests were done for each sample at each temperature. Weibull analysis was undertaken on a number of samples and this required a minimum of 15 tests.

3. Results

High temperature XRD analysis was undertaken on the interconnect materials $La_{0.7}Sr_{0.3}CrO_3$ and $La_{0.7}Ca_{0.3}CrO_3$, both synthesized by the modified Pechini method, to investigate the stability of these materials at the solid oxide fuel cell operating temperatures. The powder XRD patterns of these materials at room temperature (20 °C) and after 36 h at 1000 °C are shown in Figs 1 and 2. The XRD patterns showed that there were no observable phase changes in either material between 20 and 1000 °C. Scanning electron microscopy (SEM) analysis showed that these powders were non-agglomerated and had a uniform distribution of mean particle diameter, approximately 4 μm. A detailed particle size analysis on the LSC and LCC powders revealed that they had a narrow particle size distribution with a mean particle diameter of 3.8 μm.

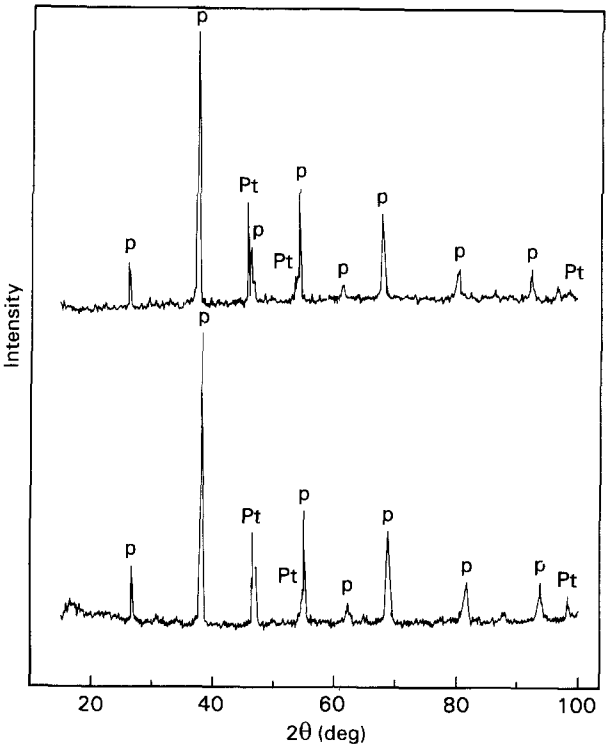

Figure 1 X-ray powder diffraction patterns of the $La_{1-x}Sr_xCrO_{3-\delta}$ sample at 25 °C (top) and 1000 °C (bottom) (p = perovskite phase; Pt = platinum holder).

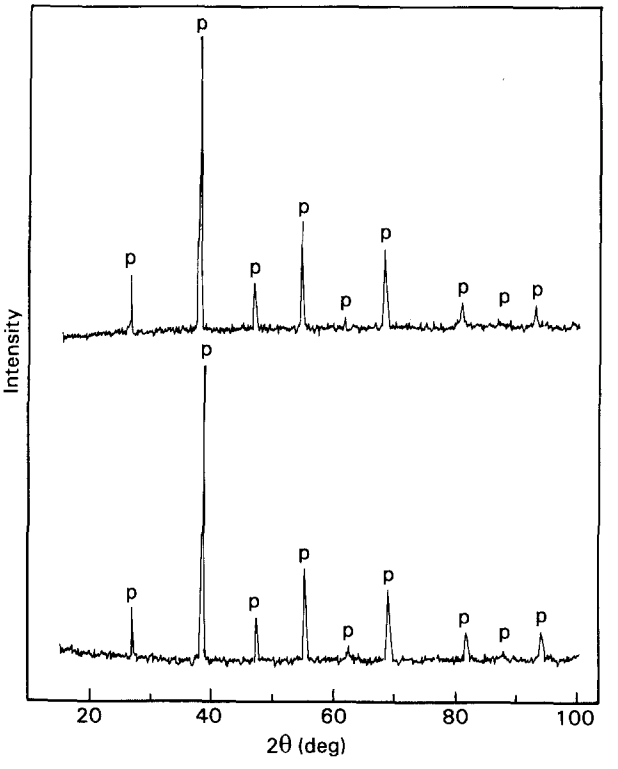

Figure 2 X-ray powder diffraction pattern of the $La_{1-x}Ca_xCrO_{3-\delta}$ sample at 25 °C (top) and 1000 °C (bottom) (p = perovskite phase).

Fig. 3 shows the effect of sintering temperature (in air) and strontium dopant concentration on the sinterability of lanthanum chromite, as a function of the percentage theoretical fired density. The powder was prepared by the modified Pechini method. The pure lanthanum chromite sample ($x = 0$) showed a poor sinterability, although the relative density was found to increase with increasing sintering temperature. The maximum relative fired density for the $LaCrO_3$ sample was found to be 64% at 1700 °C, similar to the value reported by Koc and Anderson [14]. The poor sinterability of dopant-free lanthanum chromite, when sintered in air, was due to the porosity resulting from the volatilization of chromium from the structure at high temperature. This is usually overcome by the addition of dopants such as strontia, calcia and magnesia [6]. The densification of $La_{1-x}Sr_xCrO_3$ was studied for values of $x = 0.1$, 0.2 and 0.3 as a function of temperature. The substitution of Sr for La in $La_{1-x}Sr_xCrO_3$ enhanced the sinterability over the pure $LaCrO_3$ sample. Increasing the sintering temperature, at any given composition, was found to increase the relative density. For example, the relative fired density of $La_{0.8}Sr_{0.2}CrO_3$ increased from 68 to 96% when the sintering temperature was increased from 1100 to 1700 °C. This was thought to be due to the formation of $SrCrO_3$ at intermediate temperatures, followed by melting and liquid-phase sintering [15]. The experimentally obtained relative density values indicated that there was a significant improvement in the sinterability of $LaCrO_3$ with increasing dopant concentration. A maximum relative density of 96% was obtained at 1600 °C for $La_{0.8}Sr_{0.2}CrO_3$ in comparison to 87% for $La_{0.9}Sr_{0.1}CrO_3$ sintered at the same temperature. Further increases in dopant concentration, however, did not appear to enhance the sintering characteristics of the material. These results indicated that at least 20 mol % Sr had to be substituted for La in $LaCrO_3$ in order to improve the sinterability.

The densification of $LaCrO_3$ was also investigated as a function of Ca substitution for La, as illustrated in Fig. 4. Again, the modified Pechini method was used to synthesize this powder. The substitution of Ca for La in the $LaCrO_3$ lattice again caused an increase in the sintered density of the material. For example, the substitution of 20 mol % Ca, for La in $LaCrO_3$ increased its relative density from 61 to 94% when sintered at 1400 °C. For a sintering temperature below 1500 °C, the sintered density of $La_{1-x}Ca_xCrO_3$ increased when the Ca content was increased from 10 to 30 mol %. A maximum relative density of 96% was obtained at 1500 °C for $La_{0.8}Ca_{0.2}CrO_3$, in comparison to 91% for $La_{0.9}Ca_{0.1}CrO_3$ at the same sintering temperature. However, further increase in Ca content (over 20 mol %) did not show any significant improvement in the final sintered density. It was also noted that when the sintering temperature increased

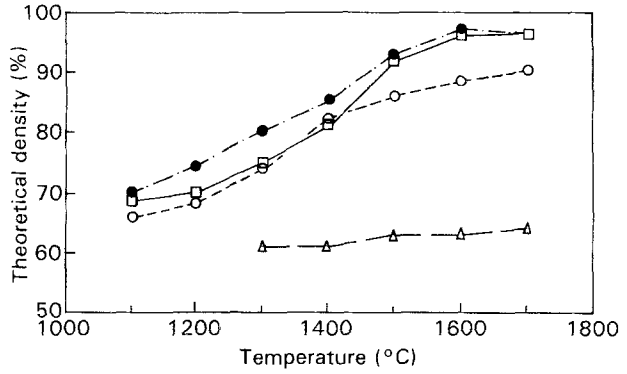

Figure 3 Sinterability as a function of sintering temperature for the strontia doped lanthanum chromite. --△--, $x = 0$; --○--, $x = 0.1$; -□-, $x = 0.2$; ·-●-·, $x = 0.3$.

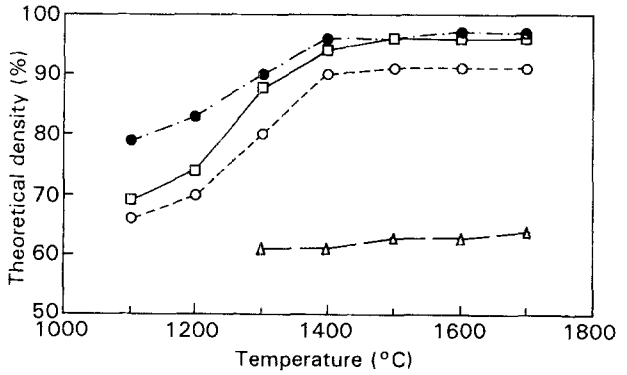

Figure 4 Sinterability as a function of sintering temperature for the calcia doped lanthanum chromite. --△--, $x = 0$; --○--, $x = 0.1$; -□-, $x = 0.2$; ·-●-·, $x = 0.3$.

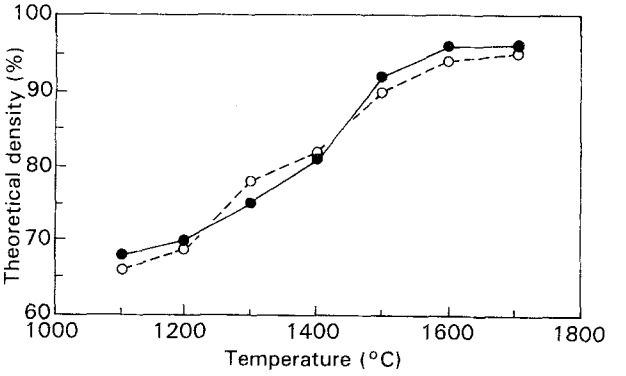

Figure 5 Effect of synthesis method on the variation of sinterability as a function of temperature for $La_{0.8}Sr_{0.2}CrO_{3-\delta}$. -●-, PM; --○--, SM.

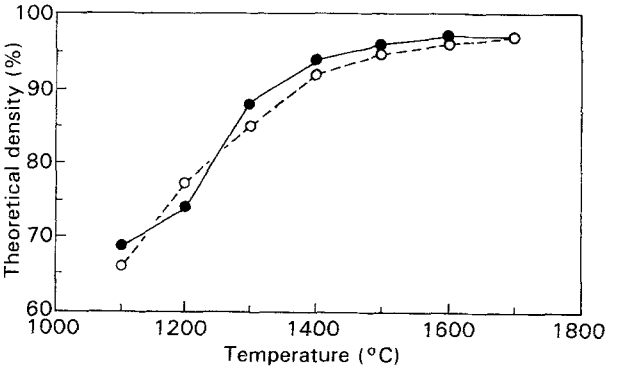

Figure 6 Effect of synthesis method on the variation of sinterability as a function of temperature for $La_{0.8}Ca_{0.2}CrO_{3-\delta}$. -●-, PM; --○--, SM.

from 1100 to 1400 °C an increase in the sintered densities was observed. This increase in the sintered density was postulated as being due to the formation of a liquid phase in this temperature range, and enhanced sinterability by liquid-phase sintering. Figs 5 and 6 show the effect of synthesis route on the sinterability of $La_{0.8}Sr_{0.2}CrO_3$ and $La_{0.8}Ca_{0.2}CrO_3$, respectively. Each material was synthesized by two different methods, namely the solid-state method and the modified Pechini method, as explained above. The observed sintered densities clearly show that the sinterability of these two materials is relatively independent of the preparation route undertaken.

Figs 7 and 8 show the effect of sintering temperature on the fracture strength of $La_{0.7}Sr_{0.3}CrO_3$ and $La_{0.7}Ca_{0.3}CrO_3$, respectively, where each material was synthesized by the modified Pechini method. The solid line indicates the variation of mean fracture strength with sintering temperature and is shown to increase with increasing sintering temperature, for both materials tested. A maximum fracture strength of 234 MPa for $La_{0.7}Sr_{0.3}CrO_3$ and 256 MPa for $La_{0.7}Ca_{0.3}CrO_3$ were obtained for both samples sintered at 1700 °C.

Figs 9 and 10 show Weibull plots of $La_{0.7}Sr_{0.3}CrO_3$ and $La_{0.7}Ca_{0.3}CrO_3$ – $\ln\ln[1/1 - F(\sigma)]$ is on the y-axis and ln (fracture strength) is on the x-axis, where $F(\sigma)$ is the median ranked stress value, given in Equation 3 (Section 4.4).

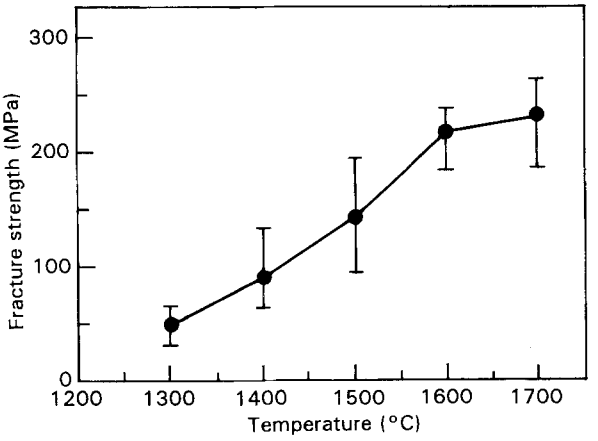

Figure 7 The fracture strength as a function of temperature for $La_{0.7}Sr_{0.3}CrO_{3-\delta}$.

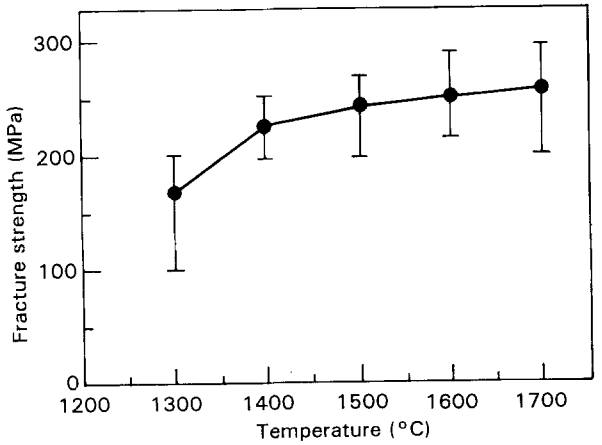

Figure 8 The fracture strength as a function of temperature for $La_{0.7}Ca_{0.3}CrO_{3-\delta}$.

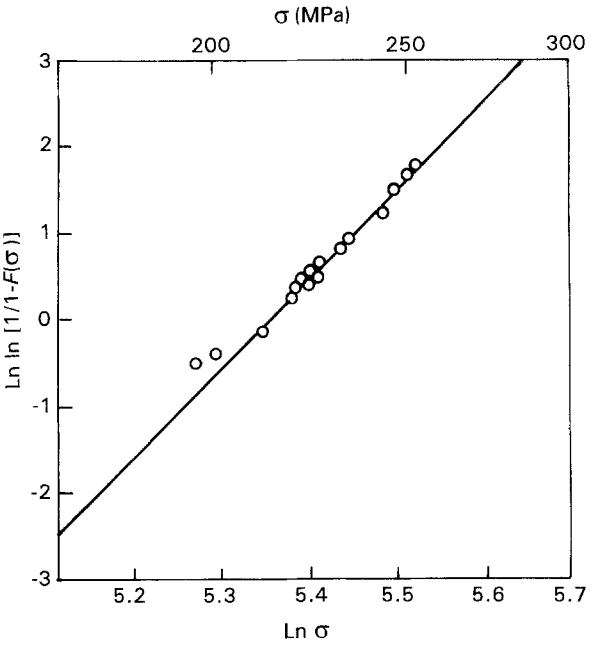

Figure 9 Weibull plot for the $La_{0.7}Sr_{0.3}CrO_{3-\delta}$ sample. σ_m = 234 MPa; m = 10.

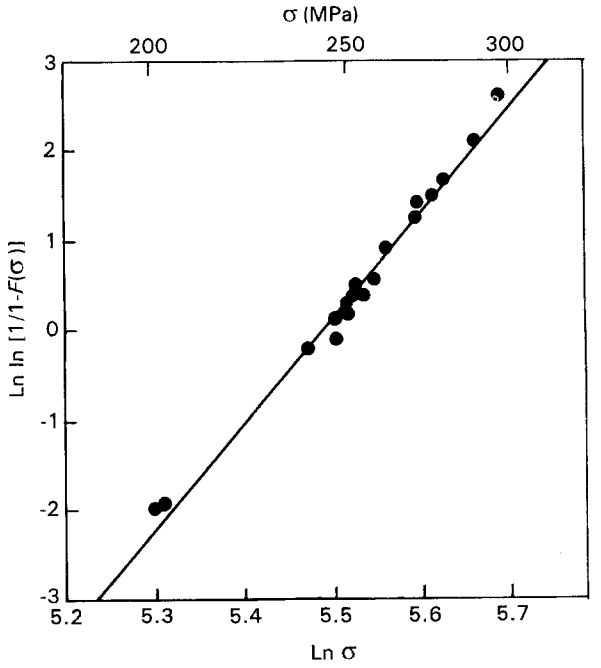

Figure 10 Weibull plot for the $La_{0.7}Ca_{0.3}CrO_{3-\delta}$ sample. σ_m = 256 MPa; m = 11.3.

4. Discussion

4.1. Powder synthesis

High temperature powder XRD data showed that both the fired LSC and LCC powders had a single orthorhombic perovskite structure at room temperature and at 1000 °C. This is shown in Figs 1 and 2 for data at 25 °C and at 1000 °C after 36 h, for the

TABLE I Comparison of the lattice parameters of the LCC samples

	Stoichiometric[a] $La_{0.7}Ca_{0.3}CrO_3$	Non-Stoichiometric[a] $La_{0.7}Ca_{0.32}CrO_3$	$La_{0.7}Ca_{0.3}CrO_3$ at 20 °C[b] ($\pm$0.01 nm)	$La_{0.7}Ca_{0.3}CrO_3$ at 1000 °C[b] ($\pm$0.01 nm)
a (nm)	0.5450	0.5452	0.5475	0.5518
b (nm)	0.5443	0.5436	0.5458	0.5507
c (nm)	0.7675	0.7689	0.7739	0.7810

[a] Data of Mori *et al.* [16]; [b] this work.

$La_{0.7}Sr_{0.3}CrO_3$ and $La_{0.7}Ca_{0.3}CrO_3$ samples, respectively. No other second phase, or phase change, was observed in the X-ray data. Hence, these materials were found to be stable under the high temperature fuel cell environments normally experienced. The extra lines in the data were due to the platinum sample holder and not to any changes in the perovskite sample.

The lattice parameters are shown in Table I and give an indication of the stoichiometry of the sample. The results of this work were compared to those of Mori *et al.* [16], which led to the conclusion that the LCC sample was not stoichiometric $La_{0.7}Ca_{0.3}CrO_3$; accordingly, the lattice parameters obtained in this work may point towards a chromium deficient $La_{0.7}Ca_{0.3}CrO_{3-\delta}$ structure. However, the authors in the above work did not analyse their powders after they had synthesized them, so there is some speculation as to the exact phase in both this work (due to the experimental accuracy) and the work of Mori *et al.* [16]. However, it could be assumed that both the LCC and LSC samples examined in this work may have been chromium deficient, even though they were stable at high temperatures. A thermal expansion value of 0.9 $\pm$ 0.09% from 24 to 1000 °C, in each axis, was calculated from the high temperature parameters.

4.2. Sintering behaviour

A general comparison of the relative density of the sintered LSC and LCC materials could be made for various dopant levels and sintering temperatures. Ninety-six percent relative density could be obtained for both $La_{0.8}Sr_{0.2}CrO_{3-\delta}$ and $La_{0.8}Ca_{0.2}CrO_{3-\delta}$ samples. However, the temperature at which the maximum relative density of 96% was obtained was higher at 1600 °C, at a constant sintering time of 5 h, for the strontia doped lanthanum chromites than for the calcia doped lanthanum chromite samples. For example, 96% density was obtained for the $La_{0.8}Ca_{0.2}CrO_{3-\delta}$ sample at 1500 °C and for $La_{0.7}Ca_{0.3}CrO_{3-\delta}$ at 1400 °C. Hence, for a 30 mol % Ca doped $LaCrO_3$ sample, 96% density could be obtained at temperatures as low as 1400 °C.

When strontia was used as a dopant in $LaCrO_3$, the increase in the sintered density was postulated as being due to the formation of $SrCrO_3$ at intermediate temperatures, followed by melting and liquid-phase sintering. The initial stages of liquid-phase sintering are thought to occur within the first 10 min after the formation of the liquid [15]. Both the rate and degree of densification increased with solid solubility in the liquid phase. During the liquid formation there was an initial rapid densification due to the capillary force exerted by the wetting liquid on the solid particles. The dominant process found in the final stages were thought to be active throughout the entire liquid-phase sintering cycle. Meadowcroft [15] observed a similar increase in the relative sintered density when the author added $SrCO_3$ to $LaCrO_3$. The author noticed that pure $LaCrO_3$ sintered very badly, and tended to degrade, and the addition of $SrCO_3$ could be used as a sintering aid, also allowing for increased physical and mechanical properties. In fact, he achieved a relative sintered density of greater than 95% for non-stoichiometric $La_{0.84}Sr_{0.16}CrO_3$ when sintered at 2027 °C in a reducing atmosphere. In this work, sintered densities of 96% could be achieved when $La_{0.8}Sr_{0.2}CrO_{3-\delta}$ was sintered for 5 h at 1600 °C in air. Tai and Lessing [9] considered that the degradation of pure $LaCrO_3$ on sintering in air was due to the following reaction:

$$2LaCrO_3 + 3/2O_2 \rightarrow 2CrO_3 + La_2O_3 \quad (1)$$

Thus, previous studies on this material were undertaken in a reducing atmosphere.

Using the same argument as mentioned earlier, although using a 30 mol % Ca doped $LaCrO_3$, it was possible that this sample may have been non-stoichiometric, due to the mobility of the Cr ion during the sintering stage. Thus, the high sinterability of the material in this work may have been due to the formation of a slightly non-stoichiometric sample. Mori *et al.* [16] showed that approximately 2 mol % Cr deficiency enhanced the sinterability of LCC. However, the authors suggested that the sinterability of the LCC material depended strongly on the chromium content and that poor sinterability was due to the formation of Cr_2O_3, as a result of vaporization from the $LaCrO_3$, and was found to decrease with decreasing sintering temperature. There is still a lot of controversy over the exact sintering mechanism of these perovskite phases and further work is currently underway to study this.

4.3. Modulus of rupture

Figs 7 and 8 show the modulus of rupture for the $La_{0.7}Sr_{0.3}CrO_{3-\delta}$ and $La_{0.7}Ca_{0.3}CrO_{3-\delta}$ samples, respectively. These materials were sintered under the conditions described above. Generally, the fracture strength increased with increasing sintering temperature for both of the examined samples. This was postulated as being due to the increase in the sinterability of the sample with increasing temperature. The LSC sample generally showed a linear increase in

fracture strength, which tailed off between 1600 and 1700 °C. The LCC sample, however, showed a large initial increase in fracture strength, at between 1300 and 1400 °C, and a very shallow increase between 1400 and 1700 °C firing temperature.

4.4. Weibull analysis

A certain degree of variability would be expected in the three-point bend tests undertaken in this work. The variability was measured by the standard deviation. The standard $\pm$ 1 deviation error encompassed approximately 68% of the observations assuming that the distribution was normal. However, this approach implied implicitly that the data behaved like a normal distribution, which may not have been a valid assumption. The Weibull distribution has an application where the above assumption cannot be met [17, 18]. The distribution follows the form of:

$$F(\sigma) = 1 - \exp[-(\sigma - \sigma_u/\sigma_0)^m] \quad (2)$$

where $F(\sigma)$ is the median ranked value; σ is the experimental test result; σ_u is the threshold stress below which the failure probability is zero; σ_0 is a scaling parameter; and m is the Weibull slope (or Weibull modulus) which characterizes the data spread.

The median rank value, $F(\sigma)$, has been calculated from $i/(n + 1)$ where i is the data value under consideration and n is the total population. This correction has been suggested [18] to account for the practical limitations of the sample size in the entire population. Often the variable σ_u is set to zero and the important parameter of interest is the Weibull modulus, m. Equation 2 can be linearized into the form of:

$$\ln\ln[1/1 - F(\sigma)] = m\ln(\sigma - \sigma_u) - m\ln\sigma_0 \quad (3)$$

σ_u was varied and the regression coefficient (R^2) was used to judge the line of best fit for the fracture strength versus sample data. In this way, σ_0 could be found from the y-axis intercept and the Weibull modulus, m, from the slope of the graph. Figs 9 and 10 show the Weibull plots for the LSC and LCC interconnect materials, respectively, after sintering at 1700 °C. Regression coefficients of 0.94 and 0.96, respectively, were obtained. The range of fracture strengths recorded for the two materials was relatively small, as indicated by the high Weibull modulus, showing that these data points were reliable for the design considerations. However, there are no other similar analyses or data points available in the literature for these materials to compare with the results of this work.

5. Conclusions

Ninety-six percent theoretical density could be achieved for $La_{0.7}Sr_{0.3}CrO_{3-\delta}$ and $La_{0.7}Ca_{0.3}CrO_{3-\delta}$ when sintered at 1700 and 1400 °C, respectively. Thus, a higher sintered density could be obtained for the latter sample at lower sintering temperatures. The mechanism for this is not yet fully understood and work is currently underway to study this further. The room temperature mechanical strengths of these materials were also measured as function of sintering temperature, and maximum strengths of 234 and 256 MPa were obtained for the two samples, respectively. Weibull analysis showed that this data was reliable for the design of the SOFC interconnect. High temperature mechanical properties are also being investigated.

Acknowledgements

The authors acknowledge the support of Fletcher Challenge Ltd, and, for the use of the high temperature XRD facilities, Industrial Research Ltd.

References

1. B. RILEY, *J. Power Sources* **29** (1990) 223.
2. A. KHANKAR and S. ELANGOVAN, *Denki Kagaku* **58** (1990) 551.
3. H. KLENSCHMAGER and A. REICH, *Z. Naturforsch* **27** (1972) 363.
4. B. K. FLANDERMEYER, M. M. NASRALLAH, A. K. AGARWAL and H. U. ANDERSON, *J. Amer. Ceram. Soc.* **67** (1984) 195.
5. S. KANEKO, T. GENGO, S. UCHIDA and Y. YAMAUCHI, in Proceedings of the Second International Symposium on Solid Oxide Fuel Cells, Luxembourg, April 1991, edited by F. Gross, P. Zegers, S. C. Singhal and O. Yamamoto (Commission of the European Communities, 1991) p. 35.
6. B. K. FLANDERMEYER, J. T. DUSEK, P. E. BLACKBURN, D. W. DEES, C. C. McPHEETERS and R. B. POEPPEL, in the 1986 National Fuel Cell Seminar, Tucson, AZ, October 1986, (Courtesy Associates, Washington, DC, 1986) p. 86.
7. S. HAYASHI, K. FUKAYA and H. SATITO, *J. Mater. Sci. Lett.* **7** (1988) 457.
8. N. SAKAI, T. KAWADA, H. YOKOKAWA, M. DOKIYA and T. IWATA, *J. Mater. Sci. Lett.* **28** (1990) 4531.
9. L. W. TAI and P. A. LESSING, *J. Amer. Ceram. Soc.* **74** (1991) 155.
10. L. A. CHICK, J. L. BATES, L. R. PEDERSON and H. E. KISSINGER, in Proceedings of the First International Symposium on Solid Oxide Fuel Cells, edited by S. C. Singhal (The Electrochemical Society, Inc., Pennington, NJ, 1989) p. 170.
11. M. M. NASRALLAH, J. D. CARTER, H. U. ANDERSON, and R. KOC, in Proceedings of the Second International Symposium on Solid Oxide Fuel Cells, Luxembourg, April 1989, edited by F. Gross, P. Zegers, S. C. Singhal and O. Yamamoto (Commission of the European Communities, 1991) p. 637.
12. B. C. H. STEELE, in Proceedings of the International Symposium on Solid Oxide Fuel Cells, Nagoya, Japan, November 1989, edited by Osamu Yamamoto (Science House Co., Ltd, Tokyo, 1989) p. 135.
13. N. M. SAMMES and M. B. PHILLIPPS, in Proceedings of the Austceram 92 Conference, Featuring Zirconia V, Melbourne, Australia, August 1992, edited by S. P. S. Badwal, M. J. Bannister and R. H. J. Hannink, (Australasian Ceramic Society, 1992) p. 49.
14. R. KOC and H. U. ANDERSON, in "Ceramic powder science III", edited by G. L. Messing, S. I. Hirano and H. Haunser, (American Ceramic Society, Westerville, OH, 1990) p. 749.
15. D. B. MEADOWCROFT, *Brit. J. Appl. Phys.* **2** (1969) 1225.
16. M. MORI, N. SAKAI, T. KAWADA, H. YOKOKAWA and M. DOKIYA, *Denki Kagaku* **59** (1991) 314.
17. S. B. BATDORF, "Fundamentals of the statistical theory of fracture", edited by R. C. Bradt, D. P. H. Hasselman and F. F. Lange, (Plenum Press, New York, 1978) p. 25.
18. B. BERGMAN, *J. Mater. Sci. Lett.* **3** (1984) 689.

Received 2 July 1993
and accepted 9 February 1994